Refractive changes with post-rotatory nystagmus in healthy individuals

Masakazu Hirota (✉ hirota.ortho@med.teikyo-u.ac.jp)
Teikyo University https://orcid.org/0000-0003-1420-9844

Ryusei Takigawa
Teikyo University: Teikyo Daigaku

Chinatsu Okabe
Teikyo University: Teikyo Daigaku

Kanako Kato
Teikyo University: Teikyo Daigaku

Ryota Nakagomi
Teikyo University: Teikyo Daigaku

Kakeru Sasaki
Teikyo University: Teikyo Daigaku

Takao Hayashi
Teikyo University: Teikyo Daigaku

Research Article

Keywords: Post-rotatory nystagmus, ocular refraction, eye movements, accommodation

Posted Date: July 22nd, 2021

DOI: https://doi.org/10.21203/rs.3.rs-189827/v1

Version of Record: A version of this preprint was published at International Ophthalmology on October 19th, 2021. See the published version at https://doi.org/10.1007/s10792-021-02028-0.

Abstract

Purpose Post-rotatory nystagmus has been used to detect autism spectrum disorders in clinical settings. Although previous studies have focused on eye movements, they did not evaluate the change in ocular refraction during post-rotatory nystagmus. This study aimed to evaluate the changes in ocular refraction during post-rotatory nystagmus in healthy individuals.

Methods A total of 34 healthy volunteers (mean age ± standard deviation, 20.9 ± 0.6 years) participated in this study. The ocular refraction during post-rotatory nystagmus was measured using MR-6000 (Tomey Inc.) on quick mode with a sampling rate of 30 Hz under noncycloplegic and cycloplegic conditions. The amplitude of post-rotatory nystagmus was calculated on the basis of the anterior eye images, while the ocular refraction measurements were simultaneously recorded. The accommodative convergence per accommodation ratio was calculated using the heterophoria method. Video oculography was performed to measure the angle of convergence during post-rotatory nystagmus.

Results The changes in ocular refraction during post-rotatory nystagmus were significantly greater under the noncycloplegic condition than under the cycloplegic condition. The changes in ocular refraction during the post-rotatory nystagmus were significantly and positively correlated with the amplitude of post-rotatory nystagmus under the noncycloplegic condition. The angle of convergence during post-rotatory nystagmus was significantly higher under the noncycloplegic condition than under the cycloplegic condition. The changes in the angle of convergence were significantly and positively correlated with the predicted accommodative convergence.

Conclusions These findings suggest that the accommodation was functional during the post-rotatory nystagmus to compensate for the retinal image slip, and the accommodative convergence can help weaken the nystagmus.

Introduction

Vestibulo-ocular reflex is the ability to stabilize the retinal image during head movement[1,2]. The endolymphatic fluid flows in the direction opposite to that of head rotation. Vestibular nuclei can be of two types; excitatory neurons and inhibitory neurons. The excitatory neurons control the ipsilateral medial rectus muscle and the inhibitory neurons control the contralateral lateral rectus muscle.

Post-rotatory nystagmus is a transient horizontal nystagmus and is induced by lymphatic movement in the lateral semicircular canal of the inner ear due to rotational arrest[3,4]. Post-rotatory nystagmus has been used to evaluate autism spectrum disorder (ASD) in the clinic. Previous studies have reported that the duration of post-rotatory nystagmus was shorter in patients with ASD than in healthy individuals[5] and that the amplitude of post-rotatory nystagmus was larger in the patients with ASD than in healthy individuals[4]. However, these studies focused only on eye movements during post-rotatory nystagmus and did not evaluate the change in ocular refraction during post-rotatory nystagmus.

The MR-6000 device (Tomey Inc., Aichi, Japan) is a new commercial autorefractometer. This instrument has an eye-tracking system that detects corneal reflection. MR-6000 measures the ocular refraction with a sampling rate of 30 Hz when the corneal reflection is present at the center of the cornea while eye tracking. Thus, the MR-6000 device can be used to measure the refractive power even if the eyes are shaking.

Prior to measuring the patients with autism using the MR-6000 device, validation studies were conducted in healthy individuals. This study aimed to evaluate the ocular refraction changes during post-rotatory nystagmus in healthy individuals.

Methods

General procedures

All study participants underwent the following ophthalmological examinations: measurement of visual acuity at a distance of 5.0 m, angle of deviation using the alternate prism cover test both at a close proximity (33 cm) and at a distance (5.0 m), and stereoacuity (Titmus Stereo Tests; Stereo Optical Co., Chicago, IL, USA). Minus and plus signs in the angle of deviation indicate exodeviation and esodeviation in the alternate prism cover test, respectively. Stereoacuity was converted to the logarithm of arcsecond (log arcsec).

Written informed consent was obtained from all participants after the nature and possible risks of the study were explained to them. This investigation was conducted in accordance with the tenets of the World Medical Association Declaration of Helsinki. The experimental protocol and consent procedures were approved by the Institutional Review Board of Teikyo University (approval no. 19-173).

Instruments

The ocular refraction was measured using the MR-6000 device, which has two measurement systems: quick mode and normal mode. The quick mode is a unique system of the MR-6000 device, and that in conjunction with the eye-tracking system is used to measure the ocular refraction with a sampling rate of 30 Hz without releasing the residual accommodation using the plus lens. The quick mode measures the refractive value using the shape of the ring image projected onto the retina. The refractive values in quick mode include off-axial aberrations within 0.6°. Therefore, the measurement error was 0.25 D for the ocular refraction within ±10 D and was 0.50 D for the ocular refraction between ±10 and ±20 D.

The accommodative target used was the balloon (visual angle, 10.5°) that was installed on Tomey's autorefractometer. During measurement, the subject was asked to fixate on the center of the balloon, which was placed at an infinite distance.

The quick mode analyzes the ocular refraction from a focal plane between a charge-coupled device camera and a fundus ring image; the ocular refractions are listed from top to bottom in order of reliability. In this study, the anterior ocular images were captured during the measurement of the ocular refraction using the quick mode in the MR-6000 device and recorded as a movie file (Movie 1). In this study, the refractive power of the right eye was measured using the quick mode, and the most reliable value among 10 measurements was converted to spherical equivalent (SE).

The normal mode is a conventional system that measures the ocular refraction after releasing the residual accommodation using the plus lens. In this study, the refractive power of the right eye was measured three times using the normal mode, and the average of the three measurements was converted to SE.

Cycloplegia

For cycloplegic eyes, two drops of 1% cyclopentolate (Alcon, Fort Worth, TX, USA) were instilled in each eye, with a 5-min interval between drops. After 45 min, the eyes were checked for dilation and pupillary response to light. The eye was considered cycloplegic if the pupil dilated to 6 mm or more and had no reaction to light. If needed, a third drop was instilled.

Experiment 1

Methods

In Experiment 1, the measurement errors between the two modes were evaluated. Twenty healthy volunteers with a mean age of 21.0 ± 0.45 (mean age ± standard deviation) years (range, 20–22 years) participated in Experiment 1. The ocular refraction was measured in quick mode and normal mode under noncycloplegic and cycloplegic conditions.

Statistical analysis

The measurement values between quick and normal modes under the noncycloplegic and cycloplegic conditions were analyzed by performing a Bland–Altman analysis[6,7]. The fixed and proportional biases between the two measurements were analyzed using the paired t-test and simple linear regression analysis.

IBM SPSS Statistics version 26 (IBM Corp., Armonk, NY, USA) was used to determine the significance of the differences, and a P-value of <0.05 was considered significant.

Results 1

The mean SE of the right eye was −3.34 ± 3.03 D. All participants had a visual acuity of equal to or greater than −0.18 logarithm of minimum angle of resolution (logMAR) with optical correction (Table 1). The average angle of deviation at a close proximity was −2.9 ± 5.4 prism diopter (PD), whereas that at a distance was −1.2 ± 2.7 PD. The stereoacuity was 1.60 log arcsec.

No significant difference was observed in the measurement values between quick (noncycloplegic, −2.86 ± 2.70; cycloplegic, −2.53 ± 2.90) and normal (noncycloplegic, −2.89 ± 2.63; cycloplegic, −2.47 ± 2.74) modes (noncycloplegic, $P = 0.80$; cycloplegic, $P = 0.60$; paired t-test) (Fig. 1a and 1b). The mean value of the differences between the two modes under the noncycloplegic condition was −0.031 ± 0.514, whereas that under the cycloplegic condition was 0.062 ± 0.458. The correlation between the two modes under the noncycloplegic condition was not significant (adjusted $R^2 < 0.001$, $P = 0.60$; simple linear regression analysis), and that the under cycloplegic condition was also not significant (adjusted $R^2 = 0.066$, $P = 0.143$) (Fig. 1c and 1d). The 95% limits of agreement under the noncycloplegic condition ranged from −0.215 to 0.278, whereas that under the cycloplegic condition ranged from −0.283 to 0.157.

Although no significant difference was found between the two modes, the refractive values that were obtained using the normal mode were considered as the baseline values that were measured before the rotation test in this study, as the variability was slightly greater in the quick mode.

Experiment 2

Subjects

In Experiment 2, we evaluated the changes in ocular refraction and the amplitude during post-rotatory nystagmus under the cycloplegic and noncycloplegic conditions. A total of 28 healthy volunteers with a mean age of 20.8 ± 0.5 (mean ± standard deviation) years (range, 20–22 years) participated in Experiment 2. A proportion of the participants were included in Experiment 1.

Rotation test

The participant was asked to sit on a rotating chair, which was placed 1.5 m away from the stationary chair, for measuring MR-6000. The rotating chair was manually rotated 20 times by an examiner (CO) in a clockwise direction under noncycloplegic and cycloplegic conditions. During the rotation test, the subject was asked to look straight ahead at another examiner's face, who measured MR-6000 once in a rotation, without the subject closing his or her eyes. The time it took for the participant to make 20 turns in each condition was recorded. The time it took to complete all 20 rotations (rotation time) was recorded.

Procedures

Figs. 2 and 3 show the procedure for Experiment 2. Under the noncycloplegic condition, the refractive power of the right eye in each participant was measured as the baseline value using the normal mode in MR-6000 (Fig. 3a). Then, the participants underwent a rotation test (Fig. 3b). Within 2 s after the completion of the rotation test, the refractive power of the right eye in each participant was measured using the quick mode in MR-6000 (Fig. 3c).

After the examination was completed under the noncycloplegic condition, the participants were given cycloplegic eye drops, and they underwent the same examination under the cycloplegic condition.

Data analysis

The change in ocular refraction was defined as the difference between the value of quick mode and baseline [quick mode – baseline].

The amplitude of post-rotatory nystagmus was analyzed from the anterior ocular images during the measurement of the ocular refraction using OpenCV 3.4.1. The original images (Fig. 4a) were converted to 8-bit grayscale images; then, median filters were applied to the grayscale images in order to delete the fonts (Fig. 4b). The binarization process was performed using a threshold value of less than 32 to adjust the brightness of grayscale images (Fig. 4c). The largest black area was determined and defined as the pupil (Fig. 4d). The eye movements were calculated on the basis of the changes in the center of pupil coordination (Fig. 5 and Movie 2). The three waveforms from the maximum to the third amplitude were determined. Each amplitude of waveforms was divided into halves. The amplitude of post-rotatory nystagmus was defined as the average of the three amplitudes of waveforms (Fig. 5).

Statistical analysis

The difference in the rotation time, the changes in ocular refraction, and amplitude during post-rotatory nystagmus between noncycloplegic and cycloplegic conditions were analyzed using a paired t-test. The correlations between the change in ocular refraction and the amplitude of post-rotatory nystagmus in both conditions were assessed by performing a simple linear regression analysis.

IBM SPSS Statistics version 26 (IBM Corp., Armonk, NY, USA) was used to determine the significance of the differences, and a P-value of <0.05 was considered significant.

Results 2

The mean SE of the right eye was −3.50 ± 2.73 D. All participants showed a visual acuity of equal to or greater than 0.0 logMAR with optical correction (Table 2). The average angle of deviation at a close proximity was −3.4 ± 5.6 PD, whereas that at a distance was −1.3 ± 2.7 PD. The stereoacuity was 1.60 ± 0.02 log arcsec. No significant difference was found in the rotation time between the noncycloplegic (27.55 ± 6.90 s) and cycloplegic (26.87 ± 5.70 s) conditions ($P = 0.30$; paired t-test). The measurement of ocular refraction was completed within 5 s.

The changes in ocular refraction during post-rotatory nystagmus were significantly and negatively greater in the noncycloplegic condition (−0.73 ± 0.71) than in the cycloplegic condition (−0.06 ± 0.27; $P < 0.001$, 95% confidence interval (CI) 0.384–0.955) (Fig. 6a). No significant difference was observed in the amplitude of post-rotatory nystagmus between both conditions ($P = 0.40$).

The changes in ocular refraction during post-rotatory nystagmus were significantly and positively correlated with the amplitude of post-rotatory nystagmus under the noncycloplegic condition (adjusted $R^2 = 0.161$, $P = 0.020$; simple linear regression analysis) (Fig. 6b); however, they were not significantly correlated with the amplitude of post-rotatory nystagmus under the cycloplegic condition (adjusted $R^2 < 0.001$, $P = 0.44$).

The result of Experiment 2 suggested that the accommodative response was functional during post-rotatory nystagmus under monocular and distant visions.

Experiment 3

Subjects

In Experiment 3, we evaluated the amplitude and frequency of nystagmus in both eyes during post-rotatory nystagmus under the cycloplegic and noncycloplegic conditions. A total of 13 healthy volunteers with a mean age of 21.0 years participated in Experiment 3. All of these volunteers also participated in Experiment 2.

Recording of eye movement

Eye movements were recorded during post-rotatory nystagmus using the Tobii Pro Nano eye tracker (T-Nano; Tobii Technology Co., Ltd., Stockholm, Sweden). T-Nano determines the eye position by detecting the corneal reflex created by the near-infrared light and compensates for 13.78" × 11.81" of freedom of head movement at 65 cm. In our pilot study, the T-Nano eye tracker was tolerant of the reflection and/or minification effects until −8.00 D. The sampling rate was 60 Hz, and the measurement angle was ± 30° from the center of the T-Nano eye tracker. T-Nano permitted the measurement at any fixation distance between 45 and 85 cm, and the measurement error was 0.2°–0.4° (interquartile range) at 65 cm.

All participants underwent a calibration test under binocular conditions prior to the fixation task because the pupillary diameter reportedly differ between monocular and binocular conditions[8], and the change in pupillary diameter affects the accuracy of eye-tracking[9].

Calibration and recording procedures were performed using the Tobii Pro software development kit with Python 3 (tobii-research 1.8.0). A small (visual angles: 0.1°) white circle drawn on a large black circle (visual angles: 1.0°) was used as the fixation target. The fixation targets were presented in front of a homogeneously gray background. During calibration, all participants were asked to fixate on five circle targets at the four corners and center of the liquid crystalline display of 12.1 inch at 50 cm. The center of the screen was described as 0.0° horizontally and vertically. The right and upper halves of the screen were defined as the positive side, whereas the left and lower halves were defined as the negative side.

After calibration, the examiner confirmed that the center of the binocular gaze position in all participants converged within the measurement error range of the T-Nano eye tracker.

Fixation task

The fixation task was performed using Python 3.6.5 on Windows. The fixation target used was the same as that used in calibration: a small (visual angles: 0.1°) white circle on a large black circle (visual angles: 1.0°). The fixation target was displayed on a gray background. During the performance of the fixation task, the participants were asked to fixate on a target for 10 s, which was displayed in the center of the liquid crystalline display, measuring 12.1 inches, at a distance of 50 cm.

The T-Nano eye tracker, placed under the liquid crystalline display, recorded the participants' eye movements.

Procedures

Figs. 7 and 8 show the procedure for Experiment 3. Under the noncycloplegic condition, the participants performed the fixation task, and the results were used as baseline values (Fig. 8a). Then, the participants underwent a rotation test (Fig. 8b). Within 2s after the completion of the rotation test, the participants performed the fixation task again (Fig. 8c).

After the examination was completed under the noncycloplegic condition, the participants were given cycloplegic eye drops, and they underwent the same examination under the cycloplegic condition.

Data analysis

Data on eye positions and pupil sizes of both eyes were exported to an Excel file. The data were excluded if the pupil diameter changed by more than 2 mm/frame because of blinking[10]. The data were also excluded if the pupil diameter changed by more than 0.2 mm/frame over an average of 11 points and a median of 5 points because of exposure to noise. A linearly interpolated value was used as a replacement for the missing values.

The mean angle of convergence was calculated on the basis of the pupillary distance and the distance between T-Nano and both eyes during the performance of a fixation task. The changes in the angle of convergence were calculated to determine the difference between the noncycloplegic and cycloplegic conditions.

The accommodative convergence per accommodation (AC/A) ratio was calculated using the heterophoria method utilizing the data of Experiment 2 and was converted from prism diopters to degrees using the following equation[11]:

$$degree = tan^{-1}(\Delta/_{100})$$

The accommodation during post-rotatory nystagmus was calculated on the basis of the difference between the changes in ocular refraction under the noncycloplegic condition and those under the cycloplegic conditions using the data of Experiment 2. Then, we predicted accommodative convergence during post-rotatory nystagmus using the following equation:

$$\begin{aligned} &predicted\ accommodative\ convergence \\ &\quad = AC/A\ ratio\ \times ocular\ refraction\ under\ the\ noncycloplegic\ condition \end{aligned}$$

Statistical analysis

The difference in the angle of convergence during post-rotatory nystagmus between the noncycloplegic condition and the cycloplegic condition was analyzed using a paired t-test. The correlations between the predicted accommodative convergence and the changes in the angle of convergence were assessed by performing a simple linear regression analysis.

IBM SPSS Statistics version 26 (IBM Corp., Armonk, NY, USA) was used to determine the significance of the differences, and a *P*-value of <0.05 was considered significant.

Results 3

The mean SE of the right eye was −3.81 ± 2.43 D. All participants showed a visual acuity of equal to or greater than 0.0 logMAR with optical correction (Table 3). The average angle of deviation at a close proximity was −4.0 ± 5.0 PD, whereas that at a distance was −2.0 ± 3.1 PD. The stereoacuity was 1.60 log arcsec. The AC/A ratio was 8.98 ± 2.50, which was calculated using the heterophoria method. The predicted accommodative convergence was 4.78 ± 3.27 PD during post-rotatory nystagmus.

The angle of convergence at the baseline was not significantly different between the noncycloplegic (24.09° ± 0.81°) and cycloplegic (23.35° ± 2.06°) conditions ($P = 0.41$; paired t-test). The angle of convergence during post-rotatory nystagmus was significantly higher under the noncycloplegic condition (25.57° ± 0.67°) than that under the cycloplegic condition (23.25° ± 1.86°; $P < 0.001$, 95% CI 0.445–1.352) (Fig. 9a). The predicted accommodative convergence (2.73° ± 1.86°) was significantly and positively correlated with the changes in the angle of convergence (2.32° ± 1.54°, adjusted $R^2 = 0.331$, $P = 0.023$) (Fig. 9b).

The results of Experiment 3 showed that the angle of convergence increased during post-rotatory nystagmus under the noncycloplegic condition. A significant positive correlation was observed between the predicted accommodative convergence and actual increase in angle of convergence; therefore, we considered that the accommodation was working during post-rotatory nystagmus.

Discussion

The present study evaluated the ocular refraction changes during post-rotatory nystagmus in healthy individuals using the high-speed autorefractometer MR-6000. The quick mode in MR-6000, combined with the eye-tracking system with a sampling rate of 30 Hz without releasing the residual accommodation using the plus lens, can measure the ocular refraction, whereas the normal mode measures the ocular refraction after releasing the residual accommodation using the plus lens under both the noncycloplegic and cycloplegic conditions (Fig. 1). Therefore, this finding suggests that the quick mode in MR-6000 is useful for measuring nystagmus and/or children with unstable fixation.

In Experiment 2, the change in ocular refraction during post-rotatory nystagmus was significantly and negatively greater under the noncycloplegic condition than under the cycloplegic condition (Fig. 5a). The change in ocular refraction during post-rotatory nystagmus was significantly and positively correlated with the amplitude of post-rotatory nystagmus under the noncycloplegic condition (Fig. 5b). These findings suggest that the accommodation is functional not only during retinal defocus but also in the retinal image slip when the retinal image slip is small. The quick mode is measured using ocular refraction, including off-axis within 0.6 degree. The measurement error of 0.25 D was determined for the ocular refraction within ±10 D and was 0.50 D for the ocular refraction between ±10 and ±20 D. Furthermore, the difference in ocular refraction between ideal position and during post-rotatory nystagmus was −0.06 ± 0.27 D in cycloplegic condition. Therefore, the measurement error in the quick mode was considered to be acceptable.

In Experiment 3, the angle of convergence during post-rotatory nystagmus was significantly higher under the noncycloplegic condition than under the cycloplegic condition (Fig. 7a); the predicted accommodative convergence was significantly and positively correlated with the change in the angle of convergence (Fig. 7b). These results support our findings in Experiment 2 and suggest that the accommodative convergence may help weaken the nystagmus.

The present study has some limitations. We could not simultaneously measure the ocular reflection and angle of convergence during post-rotatory nystagmus because the distance at the time of the ocular refraction measurement was beyond T-Nano's measurement distance. Furthermore, the sampling rate with 10 Hz of the eye camera probably underestimated the amplitude of post-rotatory nystagmus. Therefore, we plan the simultaneous measurement of the ocular reflection and both eye positions during post-rotatory nystagmus using the auto refractometer and video-oculography with a high sampling rate in the future study.

Conclusions

The ocular refraction during post-rotatory nystagmus was significantly myopic shift under the noncycloplegic condition, and it was significantly and positively correlated with the amplitude of post-rotatory nystagmus under the noncycloplegic condition. These findings suggest that the accommodation is functional during post-rotatory nystagmus to compensate for the retinal image slip; moreover, the accommodative convergence helps weaken the nystagmus.

Declarations

Conflicts of interests/Competing interests: Not applicable.

Funding: This work was supported by the Japan Society for the Promotion of Science KAKENHI Grant Numbers JP18H04116 (MH), JP19K20728 (MH), JP19K21783 (MH), and 20H04271 (MH). This work was also supported by Charitable Trust Fund for Ophthalmic Research in Commemoration of Santen Pharmaceutical’s Founder (MH) and Takeda Science Foundation (MH).

Author contributions

Substantial contributions to:

1. Conception and design: Masakazu Hirota and Takao Hayashi.
2. Acquisition of data: Masakazu Hirota, Ryusei Takigawa, Chinatsu Okabe, Kanako Kato, Ryota Nakagomi, and Kakeru Sasaki.
3. Analysis and interpretation of data: Masakazu Hirota and Ryusei Takigawa.
4. Drafting the article or revising it critically for important intellectual content: Masakazu Hirota.
5. Final approval of the version to be published: Masakazu Hirota, Ryusei Takigawa, Chinatsu Okabe, Kanako Kato, Ryota Nakagomi, Kakeru Sasaki, and Takao Hayashi.
6. Agreement to be accountable for all aspects of the work in ensuring that questions related to the accuracy or integrity of any part of the work are appropriately investigated and resolved: Masakazu Hirota, Ryusei Takigawa, Chinatsu Okabe, Kanako Kato, Ryota Nakagomi, Kakeru Sasaki, and Takao Hayashi.

Data availability: The data that support the findings of this study are available from the corresponding author (Masakazu Hirota), up on reasonable request.

Animal research: Not applicable.

Consent to participants: Written informed consent was obtained from all participants after the nature and possible risks of the study were explained to them. This investigation was conducted in accordance with the tenets of the World Medical Association Declaration of Helsinki. The experimental protocol and consent procedures were approved by the Institutional Review Board of Teikyo University (approval no. 19-173).

Consent to Publish: All authors agreement consent to publish before publication.

References

1. Raphan T, Cohen B (2002) The vestibulo-ocular reflex in three dimensions. Exp Brain Res 145 (1):1-27. doi:10.1007/s00221-002-1067-z

2. Schoene H (1964) On the Role of Gravity in Human Spatial Orientation. Aerosp Med 35:764-772

3. Howard IP, Zacher JE, Allison RS (1998) Post-rotatory nystagmus and turning sensations after active and passive turning. J Vestib Res 8 (4):299-312

4. Harrison JA, Bullock MI (1978) Post-rotatory nystagmus in hyperactive children with spatial awareness problems. Aust J Physiother 24 (4):173-180. doi:10.1016/S0004-9514(14)60878-3

5. Gresty MA, Ell JJ, Findley LJ (1982) Acquired pendular nystagmus: its characteristics, localising value and pathophysiology. J Neurol Neurosurg Psychiatry 45 (5):431-439. doi:10.1136/jnnp.45.5.431

6. Altman DG, Bland JM (1983) Measurement in Medicine - the Analysis of Method Comparison Studies. Statistician 32 (3):307-317

7. Bland JM, Altman DG (1999) Measuring agreement in method comparison studies. Stat Methods Med Res 8 (2):135-160

8. Kawamorita T, Uozato H (2014) Natural Pupil Size and Ocular Aberration under Binocular and Monocular Conditions. J Comput Sci Syst Biol 7 (1):15-19. doi:10.4172/jcsb.1000133

9. Katoh A, Hatanaka T, Takeuchi E, Uchida M, Natsume H (2015) Calibration of infrared video-oculography by using bioadhesive phosphorescent particles for accurate measurement of vestibulo-ocular reflex in mice. Journal of Advanced Science 27 (3 and 4):11-16

10. Kwon KA, Shipley RJ, Edirisinghe M, Ezra DG, Rose G, Best SM, Cameron RE (2013) High-speed camera characterization of voluntary eye blinking kinematics. J R Soc Interface 10 (85). doi:ARTN 20130227

10.1098/rsif.2013.0227

11. Irsch K (2015) Optical Issues in Measuring Strabismus. Middle East Afr J Ophthalmol 22 (3):265-270. doi:10.4103/0974-9233.159691

Tables

Table 1. Demographics of participants in Experiment 1

				Angle of deviation (PD)		
ID	Age (y)	Spherical equivalent (D)	Visual acuity (logMAR)	Near	Distant	Stereoacuity (log arcsec)
S1	20	0.00	−0.30	6	0	1.60
S2	21	−8.13	−0.30	−10	0	1.60
S3	22	−2.75	−0.30	4	0	1.60
S4	22	−0.13	−0.30	−2	0	1.60
S5	21	0.25	−0.30	−2	0	1.60
S6	21	−5.75	−0.30	−8	−4	1.60
S7	21	0.25	−0.30	−8	0	1.60
S8	21	−6.13	−0.18	−8	−8	1.60
S9	21	−2.25	−0.18	−10	−4	1.60
S10	21	−4.50	−0.18	−10	−8	1.60
S11	21	−3.00	−0.30	0	0	1.60
S12	21	−1.38	−0.30	−2	0	1.60
S13	21	−1.13	−0.30	0	0	1.60
S14	21	0.00	−0.18	−6	−4	1.60
S15	21	−6.13	−0.18	−6	0	1.60
S16	21	−3.75	−0.30	−4	0	1.60
S17	21	−7.88	−0.30	0	0	1.60
S18	20	−7.75	−0.30	4	1	1.60
S19	21	−7.13	−0.30	8	2	1.60
S20	21	0.50	−0.30	−4	0	1.60

y, years; D, diopter; PD, prism diopter; logMAR, logarithm of minimum angle of resolution; log arcsec, logarithm of arcsecond.

Table 2. Demographics of participants in Experiment 2

				Angle of deviation (PD)			Rotation time (s)	
ID	Age (y)	Spherical equivalent (D)	Visual acuity (logMAR)	Near	Distant	Stereoacuity (log arcsec)	Noncycloplegic	Cycloplegic
S1	21	−2.63	−0.30	0	0	1.60	22.39	22.88
S2	21	−1.38	−0.18	−4	0	1.60	19.71	15.27
S3	20	−2.88	−0.18	−8	−1	1.60	23.40	23.76
S4	21	−8.75	−0.18	−18	−8	1.70	21.16	22.33
S5	20	−3.88	−0.18	−6	−2	1.60	19.51	25.87
S6	20	−3.25	−0.30	−1	0	1.60	30.20	30.10
S7	20	0.63	−0.30	4	0	1.60	22.05	21.88
S8	21	−4.13	−0.30	−4	0	1.60	20.08	20.48
S9	20	0.25	−0.30	6	0	1.60	21.11	28.11
S10	21	−8.63	−0.30	−10	0	1.60	28.81	24.68
S11	22	−3.00	−0.30	4	0	1.60	28.65	24.69
S12	22	−0.75	−0.30	−2	0	1.60	23.69	23.73
S13	21	0.13	−0.30	−2	0	1.60	27.41	25.64
S14	21	−5.75	−0.30	−8	−4	1.60	24.82	20.79
S15	21	−2.38	−0.30	−8	0	1.60	32.63	31.40
S16	21	−6.25	−0.18	−8	−8	1.60	34.63	34.06
S17	21	−2.75	−0.18	−10	−4	1.60	36.87	37.87
S18	21	−5.25	−0.18	−10	−8	1.60	20.30	22.45
S19	21	−2.50	−0.30	0	0	1.60	23.86	25.67
S20	21	−3.00	−0.30	−2	0	1.60	45.04	37.10
S21	21	−0.75	−0.30	0	0	1.60	29.40	28.04
S22	21	−1.38	−0.18	−6	−4	1.60	37.36	30.96
S23	21	−5.50	−0.18	−6	0	1.60	40.09	34.84
S24	21	−3.63	−0.30	−4	0	1.60	25.19	26.72
S25	21	−8.63	−0.30	0	0	1.60	23.81	24.90
S26	20	−7.25	−0.30	4	1	1.60	26.12	25.38
S27	21	−2.63	−0.30	−4	0	1.60	23.87	22.96

S28	21	−1.38	−0.30	8	2	1.60	39.24	39.89

y, years; D, diopter; PD, prism diopter; logMAR, logarithm of minimum angle of resolution; log arcsec, logarithm of arcsecond; s, second

Table 3. Demographics of participants in Experiment 3

				Angle of deviation (PD)				
ID	Age	Spherical equivalent (D)	Visual acuity (logMAR)	Near	Distant	Stereoacuity (log arcsec)	AC/A ratio (PD/D)	Predicted AC (PD)
S13	21	0.13	−0.30	−2	0	1.60	7.60	7.60
S14	21	−5.75	−0.30	−8	−4	1.60	10.00	0.00
S15	21	−2.38	−0.30	−8	0	1.60	14.10	8.81
S16	21	−6.25	−0.18	−8	−8	1.60	6.10	3.05
S17	21	−2.75	−0.18	−10	−4	1.60	12.30	3.08
S18	21	−5.25	−0.18	−10	−8	1.60	8.10	3.04
S19	21	−2.50	−0.30	0	0	1.60	6.50	6.50
S20	21	−3.00	−0.30	−2	0	1.60	8.10	2.03
S21	21	−0.75	−0.30	0	0	1.60	6.50	0.00
S22	21	−1.38	−0.18	−6	−4	1.60	8.50	6.38
S23	21	−5.50	−0.18	−6	0	1.60	12.30	6.15
S25	21	−8.63	−0.30	0	0	1.60	6.50	4.06
S28	21	−5.50	−0.30	8	2	1.60	10.20	11.48

The participant’s ID relates with Experiment 2. y, years; D, diopter; PD, prism diopter; logMAR, logarithm of minimum angle of resolution; log arcsec, logarithm of arcsecond; s, second; AC/A, accommodative convergence per accommodation; AC, accommodative convergence.

Figures

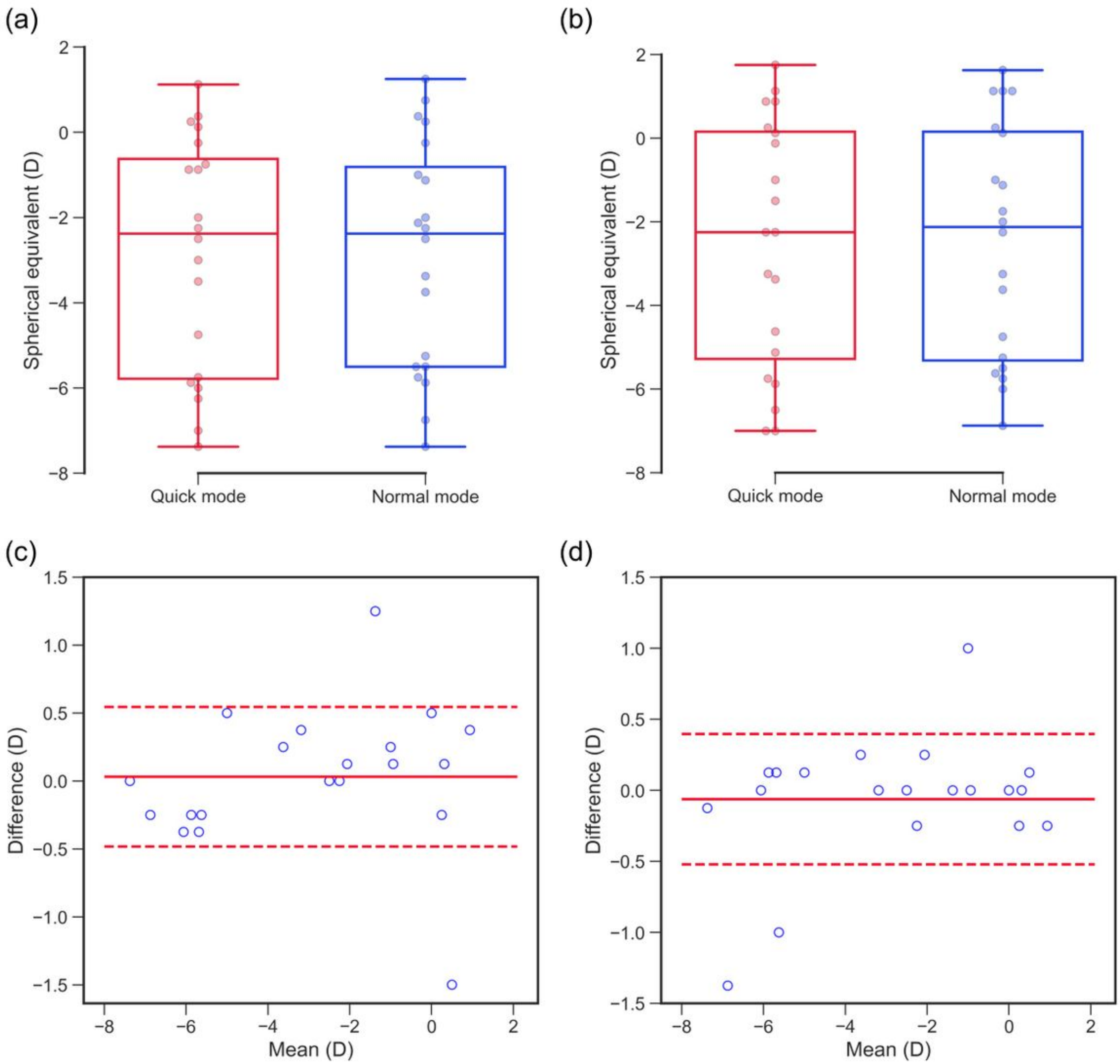

Figure 1

Comparison between quick and normal modes under the noncycloplegic (a, b) and cycloplegic (c, d) conditions. a, b: The red and blue boxplots with dots indicate the spherical equivalent (SE) using quick and normal modes. No significant difference was observed in the SE between quick and normal modes. c, d: The red solid and dashed lines indicate the mean and 1.96 standard deviation of the difference between the SE of quick and normal modes. No significant difference was observed between the two modes.

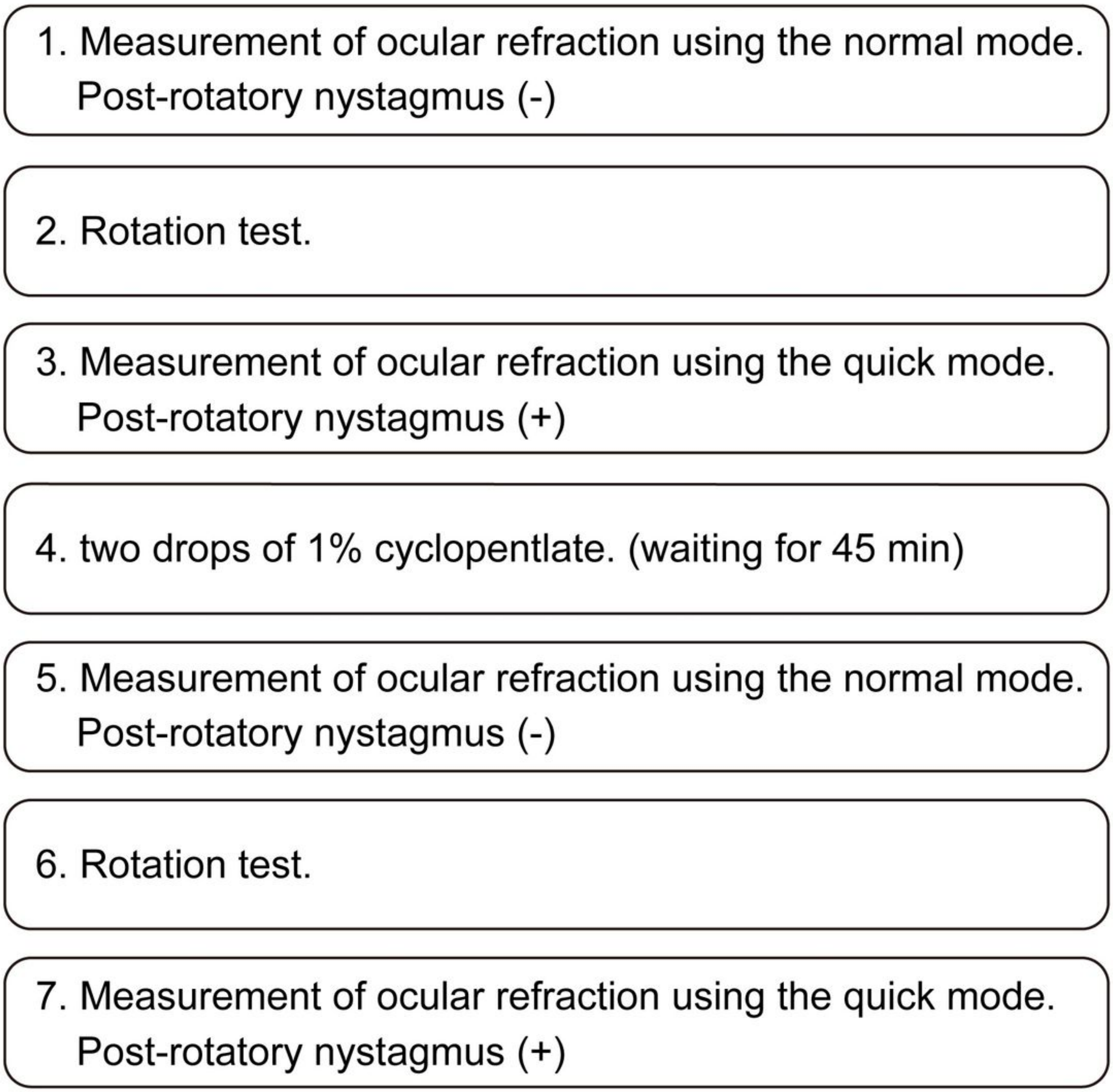

Figure 2

Procedure for Experiment 2. Under the noncycloplegic condition, the refractive power of the right eye in each participant was measured as the baseline value using the normal mode in MR-6000. Then, the participants underwent a rotation test. Within 2 s after the completion of the rotation test, the refractive power of the right eye in each participant was measured using the quick mode in MR-6000. After the examination was completed under the noncycloplegic condition, the participants were given cycloplegic eye drops, and they underwent the same examination under the cycloplegic condition.

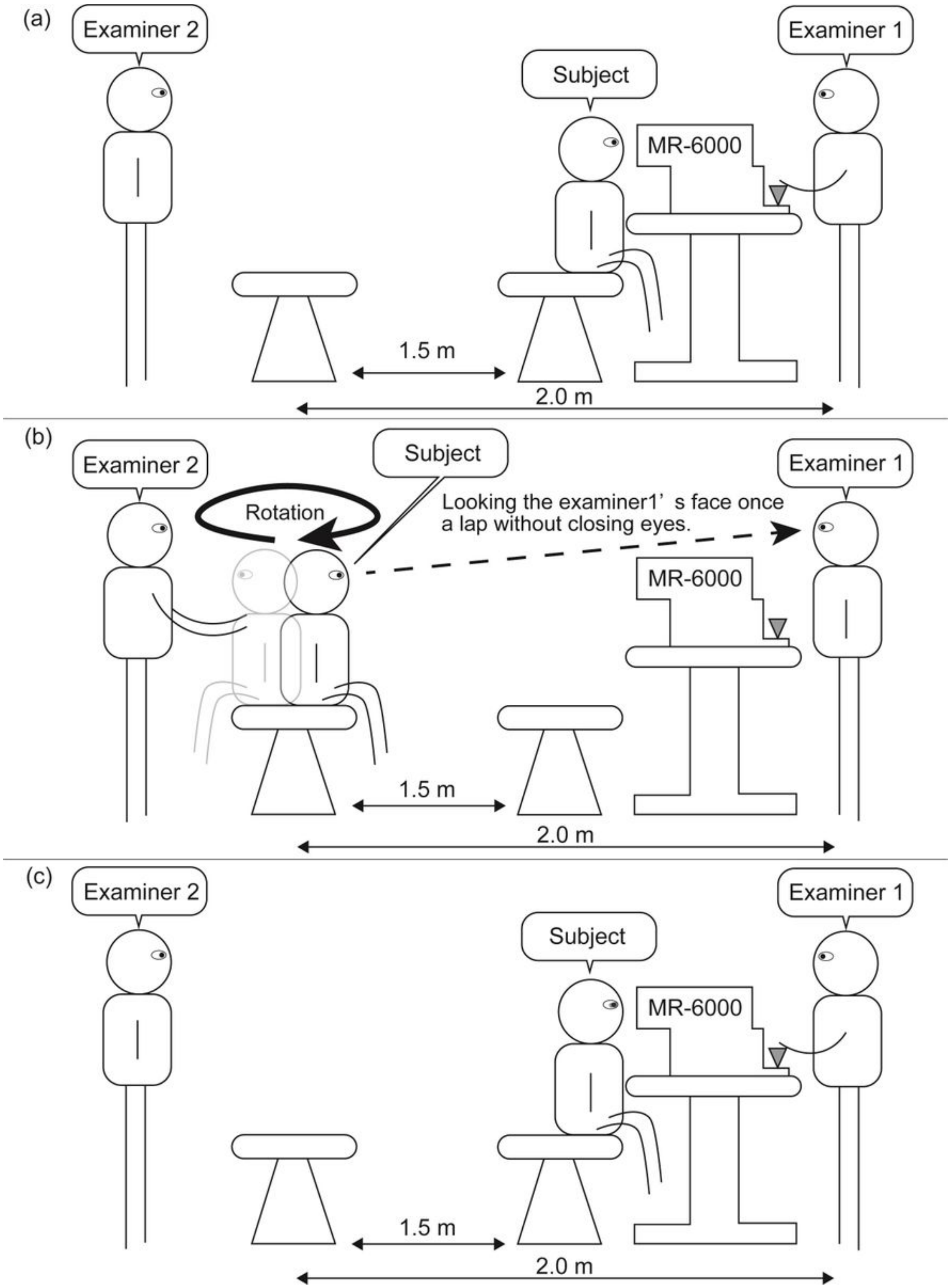

Figure 3

Measurement of ocular refraction in Experiment 2. a: The refractive power of the right eye was measured thrice as the baseline value using the normal mode in MR-6000. b: The participant was asked to sit on a rotating chair, which was placed 1.5 m away from the stationary chair, for measuring MR-6000. The rotating chair was manually rotated 20 times in a clockwise direction by an examiner. During the rotation test, the subject was asked to look straight ahead at another examiner's face, who measured MR-6000 once a lap without the subject closing his or her eyes. c: Within 2 s after the rotation test, the refractive power of the right eye was measured using the quick mode in MR-6000.

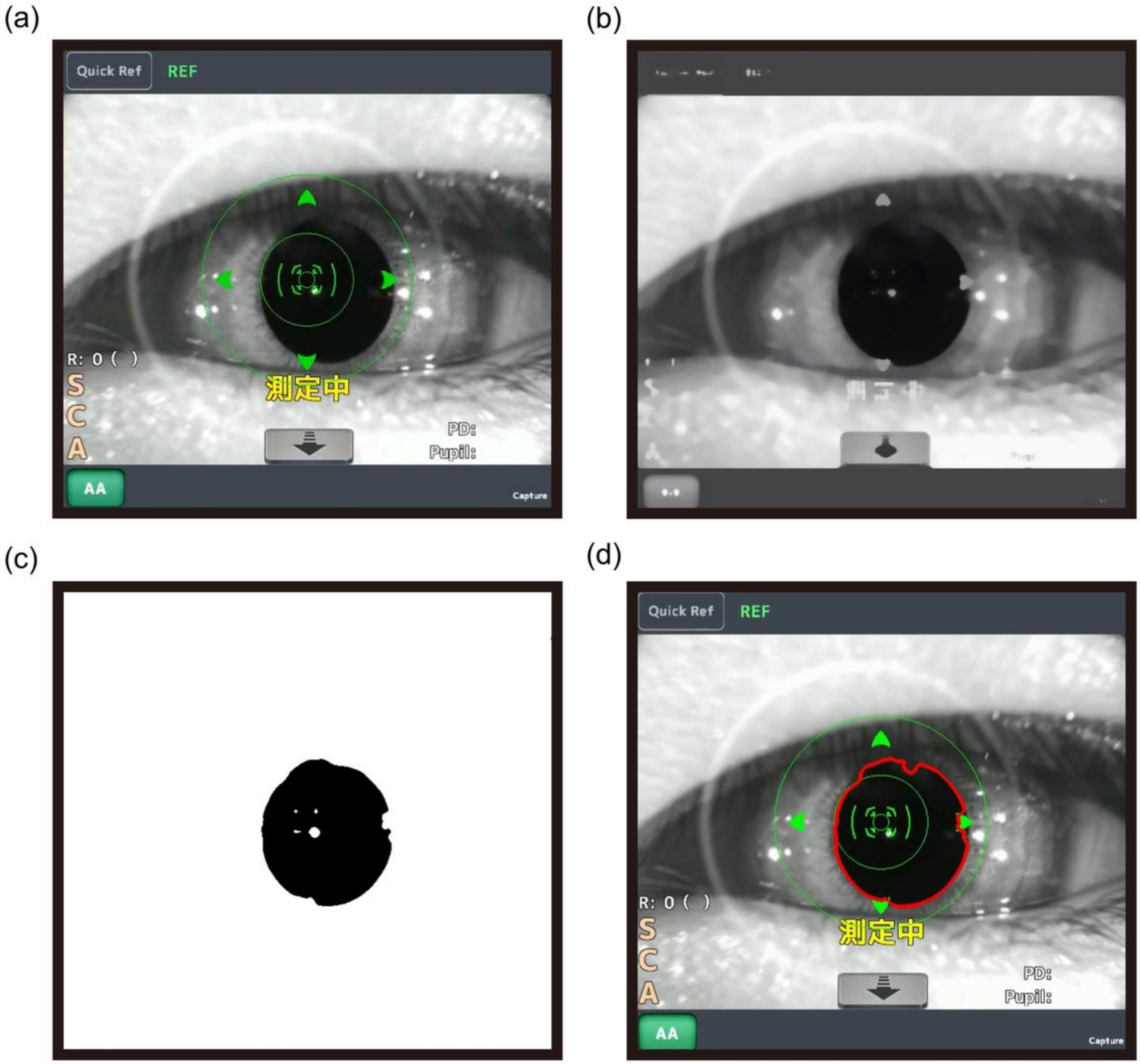

Figure 4

Image processing of post-rotatory nystagmus. The original images (a) were converted to 8-bit grayscale images; then, median filters were applied to the grayscale images to delete the fonts 2b). The binarization process was performed using a threshold value of less than 32 in the brightness of grayscale images (c). The largest black area was determined and defined as the pupil (d).

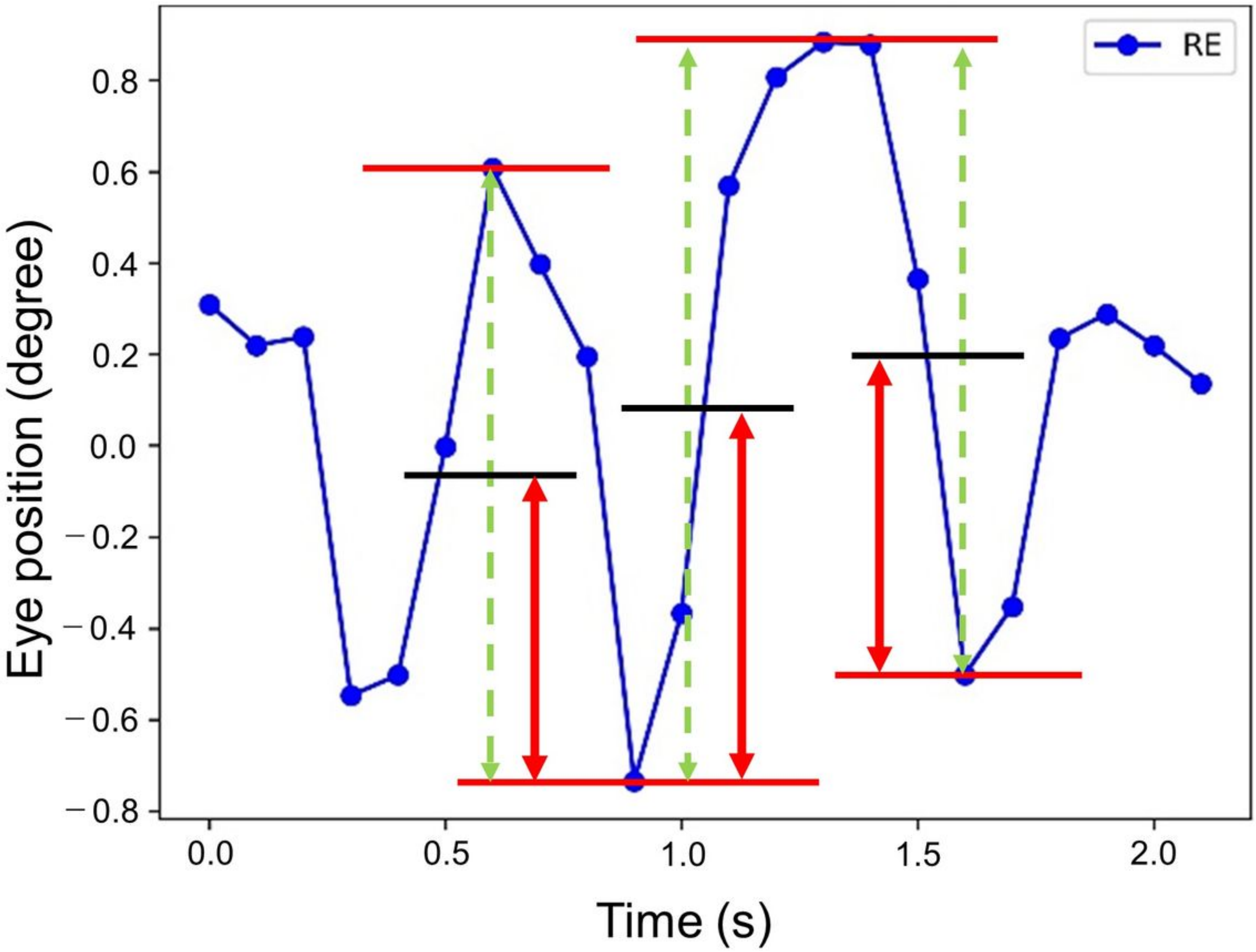

Figure 5

Calculation of the amplitude of post-rotatory nystagmus. The center of the screen in MR-6000 was defined as 0.0° horizontal. The right half of the screen was defined as the positive side, whereas the left half was defined as the negative side. The red solid lines indicate the three waveforms from the maximum to the third amplitude. The green dashed arrow lines indicate the difference in the position between the left side and right side in the right eye. The black solid lines indicate half of the green dashed arrow lines. The red solid arrow lines indicate the amplitude of waveforms. The amplitude of post-rotatory nystagmus was defined as the average of three amplitudes.

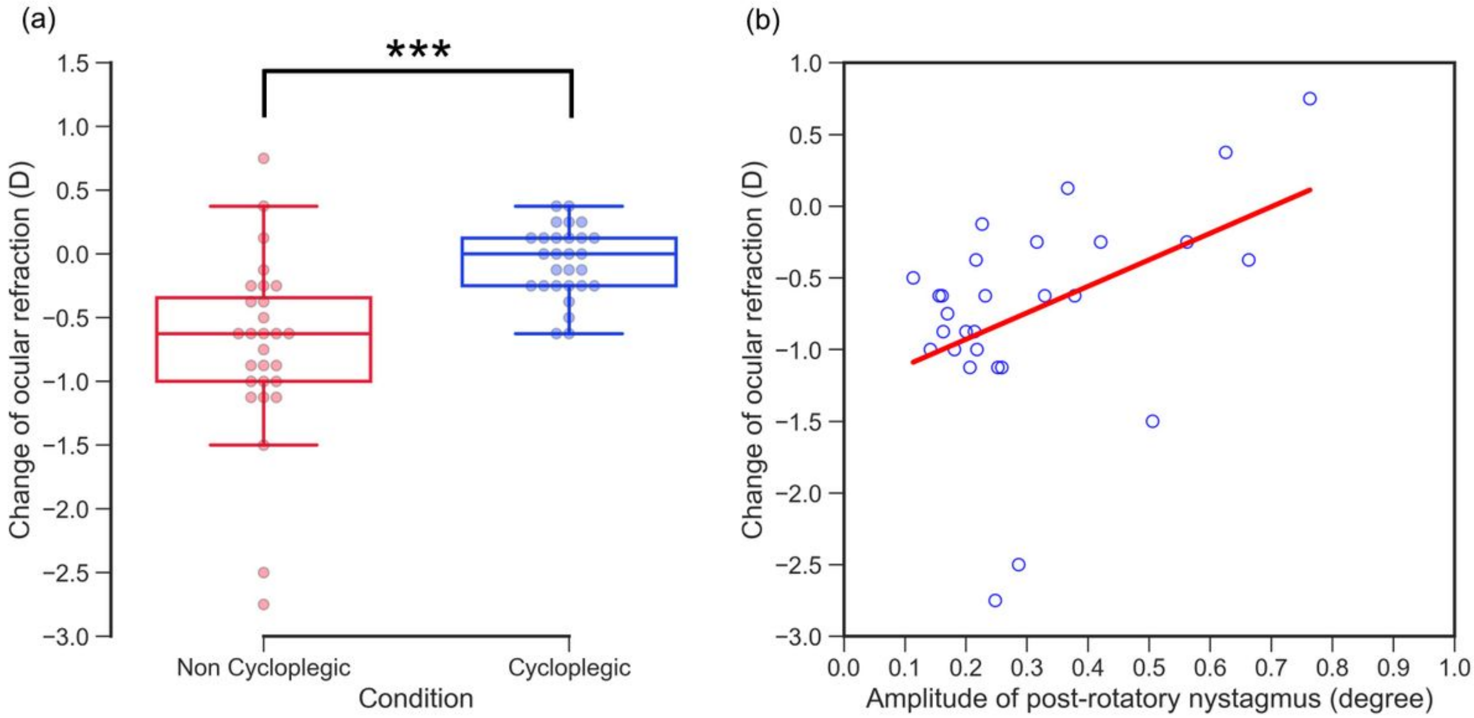

Figure 6

Change in ocular refraction during post-rotatory nystagmus (a) and its relationship with the amplitude of post-rotatory nystagmus (b). a: The red and blue boxplots with dots indicate the changes in ocular refraction under the noncycloplegic and cycloplegic conditions. The change in ocular refraction during post-rotatory nystagmus was significantly greater under the noncycloplegic condition than under the cycloplegic condition. ***: $P < 0.001$, paired t-test b: The red solid line indicates the regression line. The change in ocular refraction during post-rotatory nystagmus was significantly and positively correlated with the amplitude of post-rotatory nystagmus under the noncycloplegic condition

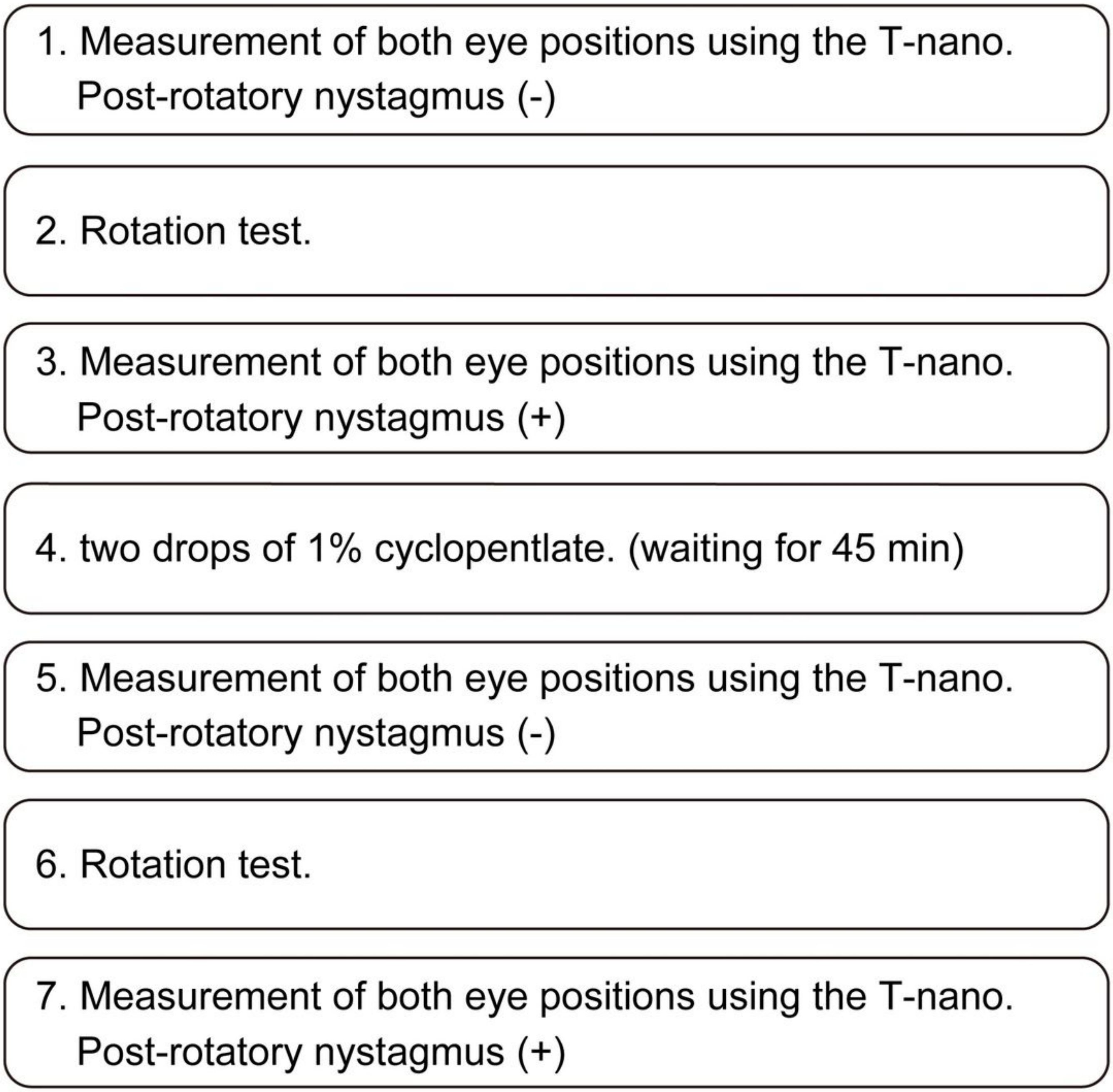

Figure 7

Procedure of Experiment 3. Under the noncycloplegic condition, the participants performed the fixation task, and the results were used as baseline values. Then, the participants underwent a rotation test. Within 2s after the completion of the rotation test, the participants performed the fixation task again. After the examination was completed under the noncycloplegic condition, the participants were given cycloplegic eye drops, and they underwent the same examination under the cycloplegic condition.

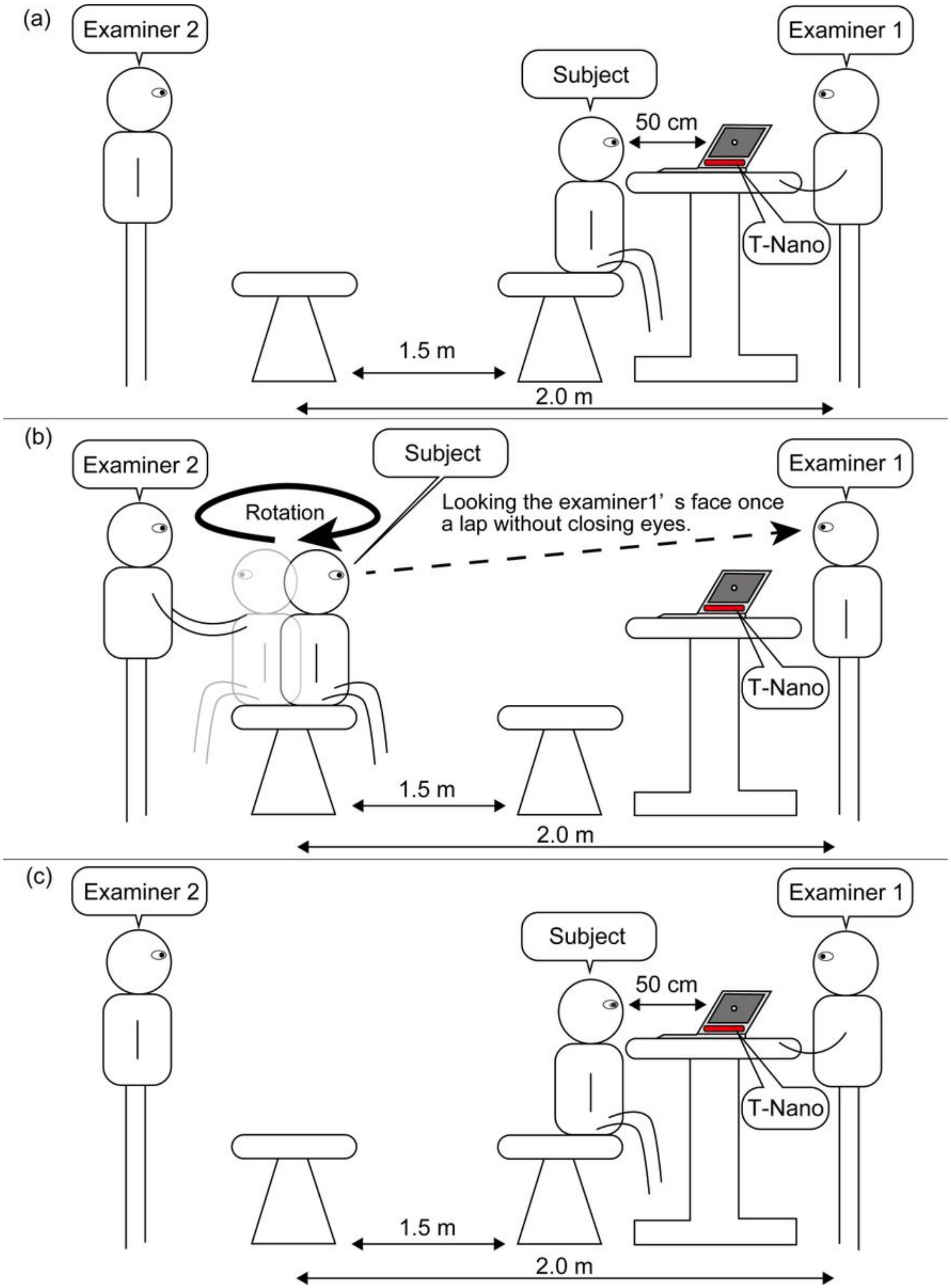

Figure 8

Measurement of both eye positions in Experiment 3. a: The participant was asked to fixate on the target for 10 s, which was at a distance of 50 cm, before the rotation test. The T-Nano eye tracker, placed under the liquid crystalline display, recorded the baseline of the participant’s eye positions. b: The participant was asked to sit on a rotating chair, which was 1.5 m away from the stationary chair, for the fixation test. The rotating chair was manually rotated 20 times in a clockwise direction by an examiner. During the rotation test, the subject was asked to look straight ahead at another examiner’s face, who recorded the eye positions once a lap without the subject closing his or her eyes. c: Within 2 s after the rotation test, the participant was asked to fixate on the target, which was at a distance of 50 cm, for 10 s. The T-Nano eye tracker, placed under the liquid crystalline display, recorded the participant’s eye movements.

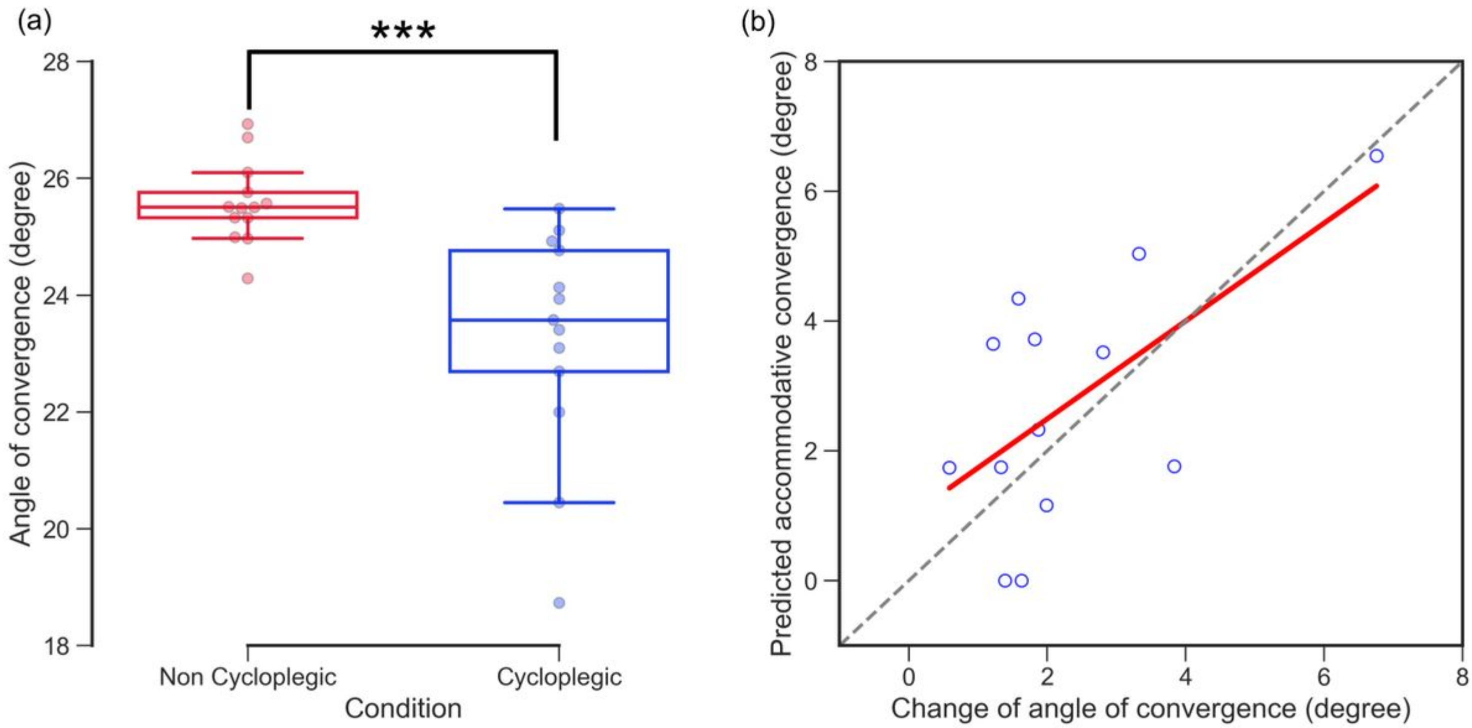

Figure 9

Change in the angle of convergence (a) and its relationship with the predicted accommodative convergence (b). a: The red and blue boxplots with dots indicate the angle of convergence under the noncycloplegic and cycloplegic conditions. ***: P < 0.001, paired t-test b: The red solid and gray dashed lines indicate the regression and equation lines. The changes in the angle of convergence were significantly and positively correlated with the predicted accommodative convergence.

Supplementary Files

This is a list of supplementary files associated with this preprint. Click to download.

- Movie1.mp4
- Movie2.mp4